EUROPEAN FUSION DEVELOPMENT AGREEMENT

EFDA–JET–PR(04)53

R. Cesario, A. Cardinali, C. Castaldo, F. Paoletti, W. Fundamenski,
S. Hacquin and JET EFDA Contributors

Spectral Broadening of Lower Hybrid Waves Produced by Parametric Instability in Current Drive Experiments of Tokamak Plasmas

Spectral Broadening of Lower Hybrid Waves Produced by Parametric Instability in Current Drive Experiments of Tokamak Plasmas

R. Cesario[1], A. Cardinali[1], C. Castaldo[1], F. Paoletti[2], W. Fundamenski[3], S. Hacquin[4] and JET EFDA Contributors[*]

[1]Associazione EURATOM/ENEA sulla Fusione, Centro Ricerche Frascati c.p. 65, 00044 Frascati, Italy
[2]East Windsor Regional School District, Hightstown, NJ 08520 USA
[3]EURATOM/UKAEA Fusion Association, Culham Science Centre, Abingdon, OX14 3DB, UK
[4]Associação EURATOM/IST Centro de Fusão Nuclear, 1049-001 Lisbon, Portugal
** See annex of J. Pamela et al, "Overview of Recent JET Results and Future Perspectives", Fusion Energy 2002 (Proc.19 th IAEA Fusion Energy Conference, Lyon (2002)).*

Preprint of Paper to be submitted for publication in
Nuclear Fusion

ABSTRACT

In order to explain the results of the non-inductive current produced in the Lower Hybrid Current Drive (LHCD) experiments, a broadening of the Radio Frequency (RF) power spectrum coupled to tokamak plasma is necessary to occur. The presented modelling, supported by diagnostic measurements, shows that the Parametric Instability (PI) driven by ion sound quasimodes that occur in the scrape-off plasma layer located near to the launcher mouth, produces a significant broadening of the launched LH spectrum. Considering the parameters of LHCD experiments of JET (Joint European Torus), and other machines as well, the PI growth rate is high enough for producing the compensation of the convective losses and, consequently, the broadening of a small fraction (≠10%) of the launched power spectrum. Such phenomenon is identified to be intrinsic of the RF power coupling in the LHCD experiments. As principal implication of considering such spectral broadening in modelling the LH deposition profile, experiments able evidencing the effects of a well-defined LH deposition profile, like those with LHCD-sustained internal transport barriers of JET, were successfully interpreted. The present work is important for addressing the long-lasting debate on the problem of the so-called spectral gap in LHCD. The design of LHCD scenarios relevant to the modern fusion research program, which require the control of the plasma current profile in the outer half of plasma, can be properly achieved by considering the PI-induced spectral broadening.

1. INTRODUCTION

The Lower Hybrid Current Drive (LHCD) [1-3] can provide a key tool for controlling the current profile in tokamak experiments aimed at achieving important goals relevant to the plasma modern research on fusion plasmas, such as the steady-state operation, improved confinement and quiescent MHD activity. In order to build such tool, a deep understanding of the physical mechanisms that determine the LH deposition profile in realistic operating conditions should be achieved. Since the LHCD effect is based on the wave interaction with a tail of the electron distribution function of plasma, the assessment of the LH power $n_{//}$ spectra that effectively propagate in the experiments is a crucial issue ($n_{//}$ is the refractive index component in direction parallel to the confinement magnetic field) [4,5]. At this regard, a long-lasting debate is still open on the so-called spectral gap in LHCD, i.e., about the causes that determine the broadening of the launched $n_{//}$ spectrum, which is necessary to occur for explaining the available experimental data by means of the quasi-linear theory [6,7,4,5].

The approach of multi-radial pass produced by ray-tracing in toroidal geometry, proposed as a cause of spectral broadening [7], has been widely accepted for modelling the LH deposition profile in LHCD experiments. However, by utilising such approach, several results observed in LHCD experiments and attributable to simple behaviours of the LH deposition with operating parameters resulted difficult to interpret [8,9]. Moreover, the precision of the modelled LHCD profile performed in Ref. [9] resulted insufficient for finding consistency with the measured current profile and the observed features of the LHCD-sustained Internal Transport Barriers (ITBs) of JET, which produced high electron temperatures in the core with broad profile [10-12].

The aforementioned problems might be correlated to some intrinsic features of the multi-radial pass approach, which make difficult determining a well defined spectral broadening and, consequently, a well defined LH deposition profile. Indeed, the utilised WKB approximation fails at the cut-off layers [5]. Conversely, at these layers, the LH waves are considered behaving like optic waves, although they have much longer wavelengths. Arbitrary choices in modelling the LH deposition profile might be thus performed in cases of the occurrence of many multi-reflections. In addition, since the spectral broadening is obtained by cumulative effects of the ray trajectories in the toroidal geometry, which in general involve the whole plasma column, the broadening results to be strongly sensitive to details of the complex magnetic structure of plasma, and to the minor changes of inputted kinetic profiles caused by experimental uncertainties as well. Therefore, assuming that the multi-radial pass is the only cause of spectral broadening, the LH deposition profile might be not a well-defined feature of an LHCD experiment and, thus, a robust tool for controlling the current profile by LHCD might be not effectively achieved. Conversely, there are indications that the LHCD produces well-defined LH-deposition profile, as occurred in the aforementioned LHCDsustained ITBs produced of JET [10-12], in which the peak of the LH-driven current density profile is localised in the outer half of plasma, consistently with the observed ITB features [9]. Therefore, it seems that the multi-radial pass approach should not fully explain the spectral broadening occurring in LHCD. Conversely, a further physics should be considered which allows improving the determination of the spectral broadening.

The model of the Parametric Instability (PI) available in the literature [13-23] provided a further cause of spectral broadening, whose consideration resulted important for obtaining well defined profiles of the driven current density in LHCD experiments performed on JET [9].

The occurrence of PIs was supported by the results of the spectra of the RF power escaping out the machine collected by probes, obtained during many experiments of the last 25 years, aimed at achieving the electron heating and CD, or the bulk ion heating in tokamaks by means of externally launched LH waves [24,20,21,22]. These experiments have been operating at relatively different plasma densities, so that $\omega_{pe} \gtrsim \omega_0$ and $\omega_{LH} << \omega_0$ or $\omega_{LH} \approx \omega_0$, respectively ($\omega_0$ is the operating frequency). The PI phenomenology evidenced the occurrence of a link between the wave physics at the edge and in the bulk plasma by means of the different plasma densities utilised in the operations. Such phenomenology should be recalled as important for better understanding the assessment of the problem of the spectral gap in LHCD, which is performed in the present work. Since the operating plasma density defines the different scenarios (for the given operating frequency), we will indicate the aforementioned experiments simply as LH experiments, thus neglecting their different goals and considering only that in these experiments the same LH wave is launched.

The PI phenomenology (see further details in the Sec.2 and Appendix I) was observed for the first time in tokamaks during LH experiments aimed at heating the bulk ions [24]. The RF probe spectra exhibited several sidebands and a broadening around the operating line frequency [20,25,21]. We indicate such frequency line broadening observed in the RF probe spectra as pump broadening

(see the Fig.1(a) of Sec 2). Modelling and experiments indicated that the multi-sideband spectra are originated by a non-linear interaction occurring at the plasma edge of the launched RF power [18,20,25,21]. The pump broadening was interpreted in terms of linear scattering by density fluctuations [26]. However, such model expects a broadening more sensitive to the plasma parameters of the bulk than of the very periphery, which is not consistent with the experimental observations indicating that the spectral broadening is a phenomenon originating mainly at the plasma edge [22]. In addition, the linear scattering model is not able providing an interpretation of the phenomenology of the RF probe and the microwave reflectometry of the plasma edge observed during the LHCD experiment on ASDEX, in which the non-linear origin of the pump broadening phenomenon was revealed [22].

In LH experiments operating at relatively high densities (in the range $\omega_{LH} \approx \omega_0$), the RF probe spectra showed both a high sideband level, often with a typical nonmonotonic envelope, and strong pump broadening (see the Fig.1 in Sec.2). In these conditions, no effect of the coupled RF power penetration in the bulk was ever observed as well. Analogously, at the relatively low operating densities proper for LHCD experiments ($\omega_{pe} \gtrsim \omega_0$, $\omega_{LH} << \omega_0$), a weak sideband activity was generally measured, but however a residual but significant pump broadening [20,25,21,27-29], non-linearly dependent on the coupled LH power [22], still persisted in the spectra. All the LH experiments treated the problem of the poor access of the coupled LH power in dense plasmas caused by strong PI activity at the edge by utilising higher operating frequencies. The highest frequency was utilised on FT, which was increased from 2.45GHz to 8GHz [30]. The access to regimes of LH interaction with the bulk plasma electrons, accompanied by RF probe spectra not exhibiting the PI cyclotron-frequencyshifted sidebands, was successfully achieved in dense plasmas, which resulted instead opaque for the LH power at same operating conditions, but lower LH frequency. However, a significant pump broadening still persisted in these experiments; in addition, it appeared stronger during experiments exhibiting a weaker effect of the coupled LH power in heating the core electrons [31]. Anyway, in all LHCD experiments equipped with RF probes, a strongly reduced PI activity accompanied the clear evidences of interactions of the LH power with the plasma electrons of the bulk. Consequently, the hypothesis that every non-linear wave interaction eventually still occurring at the plasma edge was too weak for affecting significantly the LH power propagation and deposition in the bulk was virtually, but widely, accepted. However, such hypothesis was neglecting that, in LHCD, the problems of the origin of the spectral gap and the pump broadening, as well, were still present. The present work shows that such problems are linked together much more strongly than considered in the past.

A further problem was presented by the LH experiments operating at intermediate regimes of plasma density, with respect to aforementioned regimes of bulk ion heating (not achieved) and current drive. At intermediate densities, the wave interaction with electrons disappeared and fast ion tails were observed [24]. However, no clear evidence of the LH power deposition in the bulk, comparably robust as those available in the LHCD regime, was produced. Conversely, the observed

effects on the plasma result consistent with the hypothesis of an LH deposition occurring more and more off-axis at relatively high operating density regimes, as the present paper shows.

The link between the physics of the edge of the spectral broadening and the spectral gap in LHCD was invoked for interpreting experiments of LHCD sustained ITBs in JET by means of a properly modelled LH deposition profile [9]. Following Ref [9], the present work provides further support to the occurrence of such link in the LH experiments. The consideration of the PI-induced spectral broadening in modelling the LH deposition profile is important for interpreting the aforementioned links of the LH physics of the edge and in the main plasma observed in the different LH regimes [32].

The pump broadening appears to be a peculiar feature that accompanies the launch of electrostatic waves in tokamak plasmas, as occurs in the LHCD scheme of operation. Indeed, in the other schemes utilising additional radiofrequency power (ion and electron cyclotron and resonant heating) utilising electromagnetic waves, no significant broadening of the operating frequency line was observed.

The interpretation of the LH pump broadening regards the main scope of the present paper. Following the model of the parametric instability available in the literature [13-23], extending to the LHCD operating regimes the PI analysis, which was widely performed for the early LH experiments [20-23], and analysing in details the PI phenomenon occurring in the realistic scrape-off geometries, the present paper shows that the PI provides a cause of broadening of the launched LH spectrum, which is intrinsic to the coupling of the LH power to tokamak plasmas.

The main focus of the preset paper, in summary, is that the occurrence of the PI mode coupling in the cold and overdense ($\omega_{pe} > \omega_0$) scrape-off plasma of an LH experiment, as natural feature of the electrostatic and slow waves (launched spectra with pump $n_{//peak} > 1.5$), produces a spectral broadening in the LHCD experiments consisting in the depletion of a small fraction of the pump power (≈10%). The mode coupling is driven by ion-sound quasimodes [13], which are modes of plasma that exist only in presence of a pump mode with finite amplitude. The quasimodes do not obey to a dispersion relation like the one of the normal modes involved in the PI, but only to the general conditions of the mode coupling (e.g., energy and momentum conservations). The relevant quasimodes have frequencies (in the range of 0.1MHz - 1MHz) consistent with the results of edge diagnostics performed in LHCD experiments (see Sec. II for the LHCD and the Appendix I for the different LH scenarios). For the routinely coupled LH power densities ($>$10MW/m^2), the growth rate is sufficiently high for balancing the strong energy flux losses of convective nature, which are intrinsic to the parametric instability in inhomogeneous plasmas. The PI manifests by the growth of LH sidebands with frequencies within a small shift of the pump frequency, and parallel refractive index spectrum slightly broader than the pump spectrum. The important result for the occurrence of the spectral broadening is that a higher convective loss occurs for sidebands with higher $n_{//}$ shift from the launched $n_{//}$ peak. Increasing such shift, the depletion of pump power vanishes above a certain $n_{//}$ threshold of sideband ($n_{//Sid\text{-}Cut\text{-}off}$). Higher operating plasma densities generally enhance the value of $n_{//Sid\text{-}Cut\text{-}off}$, thus enhancing the spectral broadening. The LH experiments meet, in every regime, the conditions necessary for the occurrence of the PI-induced spectral broadening, since such conditions practically coincide with those requested for performing the LH antenna

coupling, and the LH power is launched in scrape-off layers that have similar parameters in tokamaks. These conditions are: *i*) layers with $\omega_{pe} \approx \omega_0$ are located near the effective antenna-plasma interface; *ii*) the scrape-off kinetic profiles have electron temperatures ranging from a few eV to a hundred eV, and plasma densities determined, given the other parameters, mainly by the operating averaged density (roughly: $n_{eLCMS} > 0.1 n_{eAverage}$, LCMS means: last closed magnetic surface); *iii*) the scrape-off layers have typically similar radial extensions in standard tokamak experiments (≈ 3 – 6cm).

Operations at very high plasma densities, as those utilised in the early LH experiments aimed at heating the ion heating ($\omega_{LH} \approx \omega_0$), generally enhance the growth rates of PIs driven by both ion-sound and ion-cyclotron quasimodes. At the relatively low plasma densities of the LHCD experiments ($\omega_{pe} > \omega_0$, $\omega_{LH} << \omega_0$), the growth rates generally decrease, but those of the ion-sound driven PIs remain however significant. Such behaviour of the PI growth rates with the plasma density is consistent with the aforementioned phenomenology of the RF probe spectra obtained at the different LH regimes. Consequently, the link between the wave physics at the edge and in the main plasma, indicated by the LH operations at different densities, might be generally provided by the Landau damping on the plasma species, via the spectral broadening that is produced by the PIs, besides the effects of ray propagations [4]. By considering the cooperation of both the aforementioned effects in producing the spectral broadening, a more precise LH deposition profile is modelled, especially in plasmas with high central electron temperatures with broad profile, in which the LH deposition fully occurs at the first half pass [9].

The paper is organised as follows. In Sec.2, the phenomenology of the pump broadening observed on JET by RF probe and microwave reflectometry of the plasma edge is summarised. Further details on the phenomenology and the interpretation of the LH physics of the edge are given in the Appendix I. The model of parametric instability considering the parameters of an important experiment of JET [10], in which an ITB phase is sustained by performing LHCD) is summarised in the Sec.3. The PI analysis is performed: *i*) considering the homogeneous plasma limit for identifying frequencies and growth rate of the coupled modes; *ii*) performing an original calculation of the convective losses relevant to LH-induced PI driven by quasi-modes; *iii*) calculating the spatial amplification of the instability, the pump depletion and, finally, the spectral broadening. In the Appendix II, some details relevant to the plasma inhomogeneityinduced convective losses are given. In Sec.4 the operating conditions necessary for producing the spectral broadening in different LHCD experiments are identified and discussed. The Sec.5 is dedicated to the conclusions.

2. PUMP BROADENING OBSERVED DURING THE EXPERIMENT OF LOWER HYBRID CURRENT DRIVE OF JET

The RF probe measurements performed in the LH experiments operating at different regimes of plasma densities indicated that the wave physics at the edge and in the main plasma are linked via the phenomenon of the spectral broadening. In the present paper, we consider the broadening around the operating frequency observed in the probe spectra, which is referred as pump broadening. We will correlate in the next section the pump broadening to the broadening in $n_{//}$ and in frequency as

well, which is expected to occur for the launched LH spectrum, and which is refereed in the present paper as spectral broadening (i.e., both in frequency and in $n_{//}$).

As general feature of the different LH operating regimes, the spectra of the RF probes, which carry the signatures of wave interactions with the plasma, show the occurrence of a significant pump broadening, as observed e.g., on Alcator C, FT, Asdex, JT60, JET, and FTU [20,21,22,25,28,29,31].

An example of pump broadening observed during LH experiments aimed at heating the bulk ions on the FT tokamak [21] is shown in Fig.1(a). The pump broadening is measured 10dB below the power peak. Generally, in evaluating the pump broadening, the line width of the RF power generator, which is approximately of 10kHz should be excluded. The pump broadening is much bigger than such line width intrinsic to the utilised RF power sources. The ratio between the intensities of the sidebands, which appear around the operating frequency, and operating LH peak provides an equivalent evaluation of the pump broadening. The pump broadening resulted strongly enhanced operating at higher plasma densities and lower currents, which indicates that the pump broadening is directly dependent on the plasma density in the scrape-off-layer, being stronger when operating with higher scrape-off plasma densities [33,34]. As common feature of the LH ion heating experiments, which required very high plasma density of operation ($\omega_{pi} \approx \omega_0$), no penetration of the coupled LH power in the bulk occurred. In addition, besides the pump broadening, several PI sidebands shifted by the ion-cyclotron frequency of the plasma edge, exhibiting a typical non monotonic peak envelop, were observed in RF probe spectra, as shown in the Fig.1(b). A correlation was assessed between pump broadening and the typical behaviour of the PI sideband, which explained the typical shape of the peaks observed in such LH experiments. Indeed, by the modelling performed in Ref [21], the sideband behaviour occurring in the LH ion heating experiments is explained only by assuming that the LH pump that excites those sidebands has an $n_{//}$ spectrum significantly broader than the spectrum launched by the antenna. Such hypothesis of spectral broadening, necessary for explaining effects of LH power interactions with the plasma, can also explain the absence of RF penetration in the bulk due to strong Landau damping at the edge of the coupled LH power on the plasma particles. Thus the spectral broadening expected to occur in the LH experiments aimed at heating the bulk ions presents an interesting analogy with the problem of the spectral gap in LHCD, which is important for the present work. These circumstances indicate that the physics of edge and bulk are linked together despite of the differences of the LH operating regimes, regarding mainly the operating plasma densities and frequencies.

A further evidence of the occurrence of wave interactions with the plasma edge during LHCD experiments was obtained in ASDEX [22]. In this experiment, concomitant to the occurrence of spectral broadening in the RF frequency range, a broadening of the spectrum in the low frequency range of the density fluctuations was measured by microwave reflectometry of the edge.

Following, we focus on the evidences of the occurrence of frequency broadening of signals of diagnostics' measurements, relevant to the edge physics in LHCD experiments performed in JET,

performed by RF probes [28] and microwave reflectometry of the edge. An RF probe, located inside the main vessel for collecting radiofrequency power at frequencies around the operating frequency (3.7GHz), showed the occurrence of a pump broadening of about 0.2MHz (measured 10dB below the power peak) during typical LHCD experiments (operating with $<n_e> \approx 1\ 10^{19}\ m^{-3}$, $B_T \approx 3T$, $I_P \approx 3MA$), see Fig.2. Accordingly with the typical trend of pump broadening observed in different LHCD experiments [20,31,25,21,22,28,29], the pump broadening observed during LHCD experiments of JET increased up to about 1MHz when the operating with averaged plasma density was increase of about a factor two higher with respect to the case of Fig.2.

As observed in Asdex [22], a similar broadening of the spectrum in the low frequency range of the density fluctuations is observed during an LHCD experiment of JET. In this experiment, the upgraded X-mode reflectometry has been utilised [35]. One of the reflectometer systems works in the frequency range 76-78GHz, which is generally suitable to probe the plasma edge region. A proper detection allows getting the complex signal $\alpha(t).\exp[i\omega(t)]$ where $\alpha(t)$ and $\omega(t)$ are the amplitude and phase of the reflected signal respectively. The spectrum of the complex reflectometry signal is sensitive mainly to the turbulence (and then the density fluctuation) characteristics in the cut-off layer region [36]. For the considered plasma discharge performed with a magnetic field of 3.2T, the cut-off layer for the probing wave at 76GHz is located in the outer region of the plasma (around 3.8-3.9m, which corresponds to a flux radial coordinate $\rho \approx 0.98$). A fast-acquisition system is used to acquire the reflectometry signal from t=5.0s up to 6.5s with a sampling frequency of 1MHz. The considered experiment of JET utilises 2MW of LHCD power in combination of the main heating power, which is performed by Neutral Beam Injection (NBI) and Ion Cyclotron Resonant Heating (ICRH). No significant change is expected to occur in the scrape-off plasma parameters as effect of the coupling of these latter powers, which interact mainly with the plasma core. A similar broadening of the density fluctuation spectrum is observed operating in different conditions of plasmas utilising LHCD.

During this discharge, the LHCD is switched on at t=5.7s. A comparison of the spectra of the reflectometry signal before (5.0 - 5.7s) and during (5.7 - 6.4s) the LHCD phase is depicted in the Fig.3. An enhancement of the plasma density fluctuation spectrum is produced during the phase of injection of LHCD power, in the plasma edge over a wide frequency range up to the maximum detectable limit value (the Nyquist frequency is equal to 0.5MHz). This result is similar to that observed by microwave reflectometry diagnostics of the edge on ASDEX [22].

As observed during LHCD experiments on Asdex [22], the occurrence in the RF probe spectrum and microwave reflectometry measurements of a similar phenomenon of spectral broadening indicates that a non linear plasma wave interaction is produced at the edge during the LH power coupling. Such interaction is reasonably characterised by a mutual energy transfer from plasma waves at high and low frequencies. As shown in the next section, the frequency range of both the enhanced plasma density fluctuations and the pump broadening, is the same frequency range of the quasimodes driving the PI, which is relevant for the LH spectral broadening.

3. MODEL OF THE PARAMETRIC INSTABILITY FOR LOWER HYBRID CURRENT DRIVE EXPERIMENTS

The tools utilised for performing the analysis of the parametric instability (PI) relevant to the LHCD scheme for tokamak plasmas are summarised in the subsections, which is aimed at: *i*) identifying the frequencies and growth rates of the coupled modes in the limit of homogeneous plasma; *ii*) calculating the amplification factor of the parametric instability, taking into account the convective losses due to effects of both finite extent of the pump and plasma inhomogeneity, and the pump depletion which determines the broadening in the $n_{//}$ spectrum launched by the antenna (Sec.3.2). The PI model relevant to the LHCD scheme described in the classical References [15,17] has been considered for performing the analysis of the instability in the homogeneous and unbounded plasma limits. Such work has been carried out utilising the numerical tool described in Ref.[21], which achieved an interpretation consistent with the PI model for the RF-probe spectra relevant to LH experiments aimed at heating the ions. The summary of the utilised PI model and the growth rate results are shown in the Sec.3.1. The convective losses have been taken into account by performing an original analysis relevant to the PI-driven by quasi-modes (in the Sec.3.2), by utilising the formalism for PI-driven resonant modes that is available in Ref. [19]. The pump depletion and the consequent spectral broadening has been calculated (in the Sec.3.3) considering the classical work of L. Chen [16].

It is important nothing that for identifying the PI channel producing the LH spectral broadening, the search has been performed for the maximum growth rate of LH sidebands occurring in the same range of the operating frequency, imposing energy and momentum conservations of coupled modes. For a given set of plasma values, the concomitant behaviour on the growth rate has been considered of the following two important parameters: the magnetic field perpendicular component of the low frequency mode wavevector ($k_{\perp}$) that maximises the growth rate, and the angle between the perpendicular wavevectors of sideband and pump ($\delta=\angle[\mathbf{k}_{\perp}, \mathbf{k}_{0\perp}]$), which determines the group velocity direction of pump and sideband and, consequently, maximises the convective amplification factor (see the next subsection). Moreover, the search has been repeated in similar way for a further set of parameters, considering the plasma gradients.

3.1 IDENTIFICATION OF THE MODE-COUPLED FREQUENCIES AND COMPUTATION OF THE GROWTH RATE

Since the LH waves are electrostatic, the dispersion relation relevant for electrostatic coupled modes has been considered [15,19]. The PI is determined by the non-linear coupling of LH waves with low frequency modes ($\omega<<\omega_0$) of the density fluctuation background. The parametric instability of a lower hybrid pump wave $\Phi_0[-i(\omega_0 t-\mathbf{k_0}\bullet\mathbf{r})]$ is driven by a low frequency mode $\Phi[-i(\omega t-\mathbf{k}\bullet\mathbf{r})]$ and growths by two sideband waves $\Phi_{1,2}[-i(\omega_{1,2} t-\mathbf{k_{1,2}}\bullet\mathbf{r})]$, where $\mathbf{k}_{2,1}=\mathbf{k}\pm\mathbf{k_0}$, $\omega_{2,1}=\omega\pm\omega_0$. (selection rules). We assume $\mathbf{k_0}=k_{0x}\mathbf{x}+k_{0z}\mathbf{z}$, $\mathbf{k_{1,2}}=k_{1,2x}\mathbf{x}+k_{1,2z}\mathbf{y}+k_{1,2z}\mathbf{z}$, and utilise the relation $\mathbf{n}=\mathbf{k}c/\omega_0$ between refractive indexes and wavevectors. The plasma is modelled as a slab including the region of the

edge close to the antenna mouth. The *x* direction coincides with the (radial) direction of the plasma gradients, and *y, z* correspond to the poloidal and the toroidal directions, respectively. The PI analysis is based on the solution of the Vlasov and Poisson equations for coupled electrostatic modes up to the second order. The following ordering is considered: the Maxwellian distribution function corresponds to the zero order, the variation produced by the pump wave to the first order, and the perturbation of the low frequency modes to the second order ($\Phi_0 >> \Phi, \Phi_{1,2}$). The parametric dispersion relation of electrostatic coupled modes is:

$$\varepsilon(\omega, k) - \frac{{}_1(\omega_1, k_1, k_0, E_0)}{\varepsilon(\omega_1, k_1)} - \frac{{}_2(\omega_2, k_2, k_0, E_0)}{\varepsilon(\omega_2, k_2)} = 0 \qquad (1)$$

The solutions of the parametric dispersion relation, Eq.1, are the complex frequency $\omega + i\gamma$ and. where $\omega_{Re2,1} = \omega_{Re} \pm \omega_0$ and γ is the growth rate. In Eq.1, ε is the dielectric function, $\mu_{1,2}$ are the coupling coefficients referring to the lower and the upper

$$_{1,2} = \frac{\chi_e(\omega) - \varepsilon(\omega)}{\chi_e(\omega)} \frac{\omega_{pi}^2}{\omega_0} \frac{\omega_{pi}^2}{4k^2c_s^2}\left(1 + \frac{\omega}{k_z v_{the}} Z\right)^2 \sin^2 ¶_{1,2} \frac{u_2}{c_s^2} \qquad (2)$$

sidebands respectively, and are calculated considering the ion magnetised. The expression of the coupling coefficients is [17]:

The expression of the coupling coefficient is derived in the limit for $\omega \leq k_{//} v_{the}$, which is satisfied by all the solutions of Eq.1 obtained considering typical parameters of the plasma edge of LHCD experiments performed in tokamak plasmas. In Eq.2, χ_e is the electron suscectivity, c_s is the sound speed, Z is the plasma function which retains, in the performed calculations, a sum over many (≈100) ion-cyclotron frequency harmonic terms for achieving an accurate evaluation of the growth rate [14]. $\delta_{1,2}$ are the angles which the perpendicular wavevector of the lower and upper sidebands make with the perpendicular wavevector of the pump, i.e., $\delta_{1,2} = \angle(\mathbf{k}_{1,2\perp}, \mathbf{k}_{0\perp})$, and $u = ek_0\Phi_0/m_e\omega_{ce}$. The angle $\delta_{1,2}$ is one of the aforementioned important parameters for determining the strongest PI channels, since it affects the convective loss (see subsection III.2). For the geometry relevant to the wavevector components of the coupled mode, see the Fig.4, in which the only lower sideband is considered for sake of simplicity.

Considering the selections rules of the couple modes, the solutions of the parametric dispersion relation, Eq.1, are the complex frequency, $\omega + i\gamma$ and the wavevector component $k_\perp$ of the low frequency mode that drives the instability. Such solutions are determined considering all the parameters which determine the instability channel, which are: $k_{//}$, $k_{0//}$, $\delta_{1,2}$, Φ_0, B_0, n_e, $T_{e,i}$.

Due to such a high number of parameters, it is evident that performing a complete analysis of the PI relevant to a realistic experiment is a difficult task. We have performed such work by solving numerically Eq.1 and have considered different parameters of LHCD experiments. As general result,

the obtained solutions exhibit common features in the parameter ranges of LH experiments operating in a wide range of frequencies (from about 0.5GHz to 8GHz) and plasma densities ($<n_e> = 0.2 - 1\times10^{20}$ m^{-3}). Consequently, a substantially similar effect of PI-induced spectral broadening is expected to occur in the LHCD experiments. This general aspect will be discussed in the Sec. 4.

In the present section we focus to the PI analysis performed considering the aforementioned experiment producing LHCD-sustained ITBs performed on JET [10-12,9]. For a same LHCD experiment, the considered parameters of main plasma and scrape-off are shown in the Tab. I and in Fig.5, respectively. In this way, we can identify the role of the single plasma parameters in determining the PI physics, and better understand the origin of the spectral broadening in an LHCD regime. The profiles of the plasma density and the electron temperature in the scrape-off layer, in Fig.5, are obtained utilising the edge spectroscopy and the Langmuir probe measurements for the parameters of Tab. I. These profile can be considered typical for the scrape-off for operations in LHCD regime of JET, which utilise averaged line plasma densities of about 2×10^{19}m^{-3}. For higher operating plasma densities, it is worth nothing that, correspondently, in the scrape-off the plasma density increases, with profile becoming almost flat, and the temperature decreases.

TABLE I

Plasma parameters of the Pulse No: 53429 at a time point t=6.5s (during the main heating phase) which are considered for performing the model analysis. B_T= 3.4T, I_P=2.3MA, $<n_e>\approx2\times10^{19}$m^{-3}; LH power P_{LH} = 2MW, frequency f_0 = 3.7GHz, the $n_{//}$ spectrum has a peak at $n_{//0}$ = 1.84 and a width of 0.43.

Antenna dimensions: a_y = 0.864m, α_z = 0.288 m, effective radiating area: 0.816m×0.16m local toroidal magnetic field $B_T \approx$ 2.6 T.

The scrape-off has a depth $s_d \approx$ 5cm, with density and temperatures in the range (from Langmuir probes), $n_{eMin} = 0.2\div0.4\times10^{18}$m^{-3}, neMax = $2\div4\times10^{18}$m^{-3}, T_{eMin} = 5÷10eV, T_{eMax} = 20÷50eV, electron-ion temperature ratio $T_e/T_i = 1\pm0.5$.

The solutions of the parametric dispersion relation, Eq.1, obtained for a set of plasma parameters typical of the middle of the scrape-off layer (see Tab. I and Fig.5), are shown in Fig.6. This figure represents frequencies and growth rates of the low frequency modes ($\omega<<\omega_0$) that drive the PIs, and that occur in the ranges of the ionsound ($\omega\approx k_z v_{thi}$) and the ion-cyclotron harmonic ($\omega - N\omega_{ci} \approx k_z v_{thi}$) frequencies, plotted versus the perpendicular wavenumber of such modes. The highest growth occurs in the ion-sound frequency range. The following general behaviour has been found considering the different local parameters in the scrape-off. *i*) The ion-sound PI channel exhibits growth rates much higher than these of the ion-cyclotron harmonic PI channel when considering plasma parameters of layers located more in periphery (i.e., for lower plasma densities and/or electron temperatures). *ii*) The low frequency modes driving all the channels of the PIs induced by a LH pump wave in a tokamak plasma are not propagating modes, since the following condition holds:$|\varepsilon_{Re}(\omega,\boldsymbol{k})|>>1$. Therefore, the PIs are driven only by low frequency electrostatic quasimodes, heavily damped on

the plasma particles by non-linear Landau damping, due to the occurrence in tokamaks of $T_e \approx T_i$.

The PI channel driven by ion sound quasi-mode is identified, in the present work, as the most important for its implications in the LHCD experiments. Indeed, such channel involves both the lower and the upper sidebands, which are all lower hybrid waves, i.e., $\varepsilon_{Re0,1,2} \approx 0$, and exhibits very high growth rates. The presence of both sidebands is consequence of the small frequency shift of sideband and pump waves ($\omega << \omega_{ci}$), due to the very low frequency of the quasi-mode that drives the instability. Conversely, for the ion-cyclotron quasi-mode driven channel (which however has a lower growth rate in the considered LHCD parameter regime), only the lower sidebands are propagating LH waves (i.e., $|\varepsilon_{Re2}| >> 1$).

Focusing now only on the ion-sound-driven PIs, the trend of the growth rate maxima with respect to $k_\perp$ of the driving quasimode has been determined considering different local parameters within the scrape-off layer (see Fig.5). The effect of the plasma gradient in the scrape-off on the growth rates is shown the Fig.7, where the growth rate is plotted against the local plasma density keeping in one case the electron temperature as fixed parameters, and in the other accordingly with the plasma gradient (as in the Fig.5). It is evident the effect of reduction of the growth rates increasing the local electron temperature (T_e>0.1keV). Such reduction becomes very strong in the layers located inside the separatrix due to the building of the T_e step gradient. The strongest PI ($\gamma/\omega_0 \approx 0.02$) occurs in the layer with low temperature ($T_e \lesssim 10$eV) and density ($n_e \approx 2\times10^{17} m^{-3}$) close the LH cut-off density ($\omega_{pe} = \omega_0$), which is reasonably located near the launcher-plasma interface. The trend of the real frequency of the quasimode (frequency shift from the pump) and the growth rate with the major radius is summarised in the Fig.8. The error bars in the growth rates take into account the experimental uncertainties due to the measured scrape-off profiles (a factor two on the plasma density and temperature in a given layer), and reveal a relatively small dependence of the growth rate on the input parameters, e.g.: $\Delta\gamma/\gamma \approx -5\%$ for T_e increased of a factor 2). We understand such behaviour considering that a quasimode with proper parameters (wavenumber and frequency) is however available in a given layer for producing a strong mode coupling (see also Sec.3.2). As shown in Sec.4, profiles of maximum growth rates of ion-sound-driven PIs similar than the one shown in Fig.8 represent a common feature of the LHCD experiments.

Regarding the PI channels driven by the ion-cyclotron quasi-modes (not shown in the Fig.8), for LHCD plasma parameters, they have growth rate lower than that of the ion-sound driven channel, especially in the very periphery, and require a much higher operating plasma densities (so that ω_{LH}/ω_0, ≈ 0.03) for becoming of significance ($\gamma/\omega_0 \approx 10^{-2}$). Such high densities regimes of are generally not achieved in the LHCD operations, since not significant current fractions are obtained.

Now, we can focus on the spectral features of the LH sidebands growing in the PI, since they might produce the searched broadened LH spectrum that penetrates in the bulk. At this regard, the behaviour of the growth rate with respect to the $n_{//}$ of the lower sideband is plotted in Fig.9, assuming as parameters two values of plasma densities typical of the scrape-off (the others parameters have been kept fixed). A similar trend (not shown here) is found considering the upper sideband. This

figure indicates that the instability might grow in LH sidebands (which have a small shift in frequency with respect to the operating frequency, $Re(\omega)/\omega_0 \approx 5\,10^{-4}$, and a significant growth rate, $\gamma/\omega_0 \approx 2\,10^{-3}$) over a wide range of sideband $n_{//}$ (up to the maximum considered value, corresponding to about two times the pump $n_{//}$).

Therefore, the PI phenomenon can in principle broaden both the frequency and $n_{//}$ spectra coupled by the launcher. For ascertaining if the phenomenon can actually take place, the convective nature of the instability must be now properly considered.

3.2 *CONVECTIVE LOSS AND SPATIAL AMPLIFICATION OF THE PARAMETRIC INSTABILITY*

In the present subsection we identify the conditions that determine the occurrence of the parametric instability considering its nature of convective instability, in the realistic case of an LHCD experiment. We focus here on the determination of the amplification factor of the parametric instability, which is necessary for the computation of the fraction of pump power going to the sidebands. The results of the consequent spectral broadening will be presented in the next subsection.

The approximations of unbounded and uniform plasma, utilised in the growth rate homogeneous analysis of Sec 3.1 should be removed for taking into account the convective losses. In a first step, the LH wave energy flux contained in well defined resonant cones in a magnetised plasma [14,37] is considered for obtaining the PI amplification factor in the limit of finite extent of the pump (A_{FEP}) [19]. The characteristic scalelength of the PI is thus determined, and the effect of the plasma inhomogeneity can be included. As main result, we will show that the plasma in homogeneity inhibits the growth of the sidebands, especially for those with a higher $n_{//}$ shift from the pump.

The present analysis has been performed following Ref [19] and is organised as follows: *i)* the finite extent of the pump region is considered in slab geometry for evaluating the threshold of the pump power density and the radial extension of the region of PI, *ii)* the effect of plasma inhomogeneity producing a phase mismatching between coupled modes is considered. In the analysis, only the lower sideband is considered for the sake of simplicity; however, the extension of the analysis to the upper sideband is straightforward.

We consider the slab geometry, shown in Fig.10, which indicates the group velocities of pump and sideband (for simplicity only the lower sideband), and the propagating regions of their energy fluxes. The ξ direction is that perpendicular to the pump group velocity, and x, z indicate, as used, the directions of the plasma gradients and confinement magnetic field, respectively. The wave potential can be considered uniform in the region illuminated by the antenna, $\Phi_0 = P_0$ for $0 < \xi < L$ and $\Phi_0 = 0$ otherwise. At the boundary, $\Phi_0 = P_0$ for $0 < z < 2a$ and $\Phi_0 = 0$ otherwise $2a$ is the dimension of the antenna in the toroidal direction. The sideband potential, which corresponds to thermal fluctuations, is $\Phi_1 = P_1$ for all z. The onset of the convective instability is conditioned by the occurrence of a positive balance between the rate of energy gained by the sideband from the pump and the one lost in convection. The exponential amplification factor characterising the spatial growth

of the parametric instability considering the effect of the finite extension of the pump region is:

$$A_{FPE} = \frac{\gamma(k_1, E_0, \omega_0, \omega_1)L}{v_{g1\xi}} \tag{3}$$

where γ is the growth rate, L is the width of the pump region in the x, z plane, $v_{g1\xi}$ is the group velocity component of the sideband in the direction perpendicular to that of the pump [15,19]. The occurrence of significant PI requires that the amplification factor is A>1, which produces the threshold in the electric field of the pump. As general feature of the PI, the homogeneous growth rate is maximised by values of the angle $\delta_1 \equiv \angle(\mathbf{k}_{1\perp}, \mathbf{k}_{0\perp}) \approx \pi/2$; conversely, small angles that make almost aligned the pump and sideband group velocities reduce the convective loss. The trend of the PI amplification factor, calculated considering the homogeneous growth rate obtained in the previous subsection, is plotted against the angle δ_1 in the Fig.11, and allows determining the optimum angle for higher amplification factor. The maximum amplification factor occurs for small angles of the pump and sideband k-vectors ($\delta_1 \approx 10°$). In this conditions we have obtained, referring to the geometry in Fig.9: $_{vg1\xi}/c \approx 1\ 10^{-3}$ (with, typically: $v_{g0,1x}/c \approx 0.15$, $v_{g0,1z}/c \approx 0.4$). Therefore, for determining the amplification factor A_{FPE} we have solved Eq.3 assuming $\delta_1 = 10°$, and repeated the calculation for plasma parameters relevant to different radial positions in the scrape-off. Some indicative values obtained in the middle of the scrape-off and utilised for calculating the PI amplification factor, by solving Eq.3, are: $\gamma/\omega_0 \approx 1.5\ 10^{-3}$, which give $A_{FPE} \approx 9$.

It is interesting determine the radial size Δx of the PI interaction layer, in which $A_{FPE} > 1$ holds, and convective loss due to pump finite extent thus should allow the growth of the PIs. Considering the dependence of the growth rate on the kinetic plasma profiles, we have found: $\Delta x \approx 5$cm, i.e., which Δx has roughly the same dimension of the scrape-off layer. It means that the growth of the PIs can occur only in the scrape-off layer, as reasonable since the temperature step gradient occurring inside the LCMS strongly reduces the growth rates of the PI interaction layer, in which the condition $A_{FPE} > 1$ is satisfied, has been determined. As result, Δx coincides roughly with the dimension of the scrape-off layer, i.e. $\Delta x \approx 5$cm.

The contribution of weak plasma inhomogeneity to the convective loss can be now determined following Refs. [19,23]. The WKB analysis has been performed considering the origin at the interaction point x=0 (see Fig.9), in which the k-matching condition of the coupled modes holds: $\mathbf{M}$"a$\mathbf{k}$-$\mathbf{k}_0$-$\mathbf{k}_1$=$\mathbf{0}$. Away from this point, the phase mismatching $M \neq 0$ due to the plasma inhomogeneity determines the convective loss. Expanding away from x=0 and considering that the plasma parameters change only in the x direction, $M_y \equiv M_z \equiv 0$, and the component $M_x \equiv k_x - k_{0x} - k_{1x}$ can be expressed as:

$$M_x - \frac{dM_x}{dx}\Big|_{x=0} dx \tag{4}$$

For determining M_x and, consequently, the convective loss due to the plasma inhomogeneity, we consider the following arguments. *i*) A lower limit holds for M_x ($M_{xMini} \approx 1/\Delta x \approx 0.2\text{cm}^{-1}$) imposed by the scalelength of the instability; *ii*) The condition of frequency matching $\omega - \omega_0 - \omega_1 \equiv 0$ occurring at the interaction layer should be maintained also away from the point $x = 0$. For satisfying this condition we consider the features of the coupled modes. About pump and sideband, we know that they are LH waves propagating radially inwards in regions with higher densities, and that the expression of the"*x*"component of the wavevector can be obtained utilising the lower hybrid dispersion relationship

$$k_{0,1\perp}\,\omega\ \ \frac{\omega_{LH}}{\omega_0}\,k_{0,1//}\sqrt{\frac{m_i}{m_e}} \tag{5}$$

Conversely, no limitation (like one imposed by a dispersion relation) occurs for the low frequency quasi-mode (the only limitation being that it can exist only in presence of a pump with finite amplitude). *iii*) The aforementioned minimum phase mismatching, M_{xMini}, occurs for a sideband with spectral characteristics similar then the pump, i.e., with $k_{1z} \approx k_{0z}$. Consequently, for the radial component of the quasi-mode wavevector, the condition $k_x \approx 2k_{0x}$ holds, and the expression $M_x \approx k_{0x}\text{-}k_{1x}$, for the *k*-matching condition, is obtained for performing the following WKB analysis. We note that all the aforementioned solutions of Eq.1 have the wavenumbers of the coupled modes consistent with such condition (see also the Appendix 2), which indicates consistency between the homogeneous and inhomogeneous analyses.

The coupled equations of the sideband wave and of the quasi-mode potentials are:

$$\left(\frac{\partial}{\partial t}+v_{g1x}\ \ \frac{\partial}{\partial x}+\Gamma_1\right)\Phi_1=-i\frac{\alpha_1}{\partial\varepsilon_{1R}/\partial\omega_1}\,\Phi\,e^{i\int M_x dx} \tag{6}$$

$$\left(\varepsilon+i\frac{\partial\varepsilon}{\partial\omega}\ \frac{\partial}{\partial t}\ -i\ \frac{\partial\varepsilon}{\partial k_x}\ \frac{\partial}{\partial x}\right)\Phi\ =\alpha\Phi_1 e^{i\int M_x dx} \tag{7}$$

where: $\alpha=\varepsilon\Phi/\Phi_1$, $\alpha_1 = \varepsilon_1\Phi_1/\Phi$, Γ_1 is the linear damping of the sideband wave and the subscript *R* indicates the real part. Utilising the expressions [19]:

$$\Phi = p e^{-i\frac{dM_x}{dx}\frac{x^2}{4}} \tag{8}$$

$$\Phi_1 = p_1 e^{i\frac{dM_x}{dx}\frac{x^2}{4}} \tag{9}$$

Eqs. 9 and 10 can be integrated obtaining the spatial evolution of the sideband:

$$p_1(x) = p_{10} e^{\frac{\gamma\pi}{\frac{1}{\varepsilon_I}\frac{\partial\varepsilon_R}{\partial k_x}\frac{dM_x}{dx} v_{g_{1x}}}} \tag{10}$$

The amplification factor due to plasma inhomogeneity is:

$$A_{INHOM} = \frac{\gamma\pi}{\frac{1}{\varepsilon_I}\frac{\partial\varepsilon_R}{\partial k_x}\frac{dM_x}{dx} v_{g1x}} \tag{11}$$

where the subscript *I* indicates the real part. Utilising the relation $M_x \approx k_{0x}$-k_{1x}, the amplification factor containing the effect of plasma inhomogeneity can be expressed in term of parallel refractive index shift of the sideband and pump:

$$A_{INHOM} = \frac{\gamma\pi}{\frac{1}{\varepsilon_I}\frac{\partial\varepsilon_R}{\partial k_x} v_{g1x} D \cdot (n_{1//} - n_{0//})} \tag{12}$$

where *D* is a factor depending on the plasma density profile.

Therefore, considering both the convective losses due to the effects of finite pump extent and plasma inhomogeneity, the amplification factor of the parametric instability is given by:

$$A = \min(A_{FEP}, A_{INHOM}) \tag{13}$$

Considering the related behaviour of the growth rate and the plasma density profile in the scarpe-off:

$$n_e(x) = n_{e0} e^{\frac{x}{\lambda}} \tag{14}$$

where n_{e0} is the density at the layer $\omega_{pe} \approx \omega_0$, the amplification factor is plotted in Fig.12 versus the parallel refractive index of sideband. The trends of A_{FPE} and A_{INHOM} are also indicated. In addition, the ray-tracing has been utilised for determining more accurately the radial size of the interaction region and, consequently the convective loss due to plasma inhomogeneity. The result is indicated by the term $A_{INHOM+RT}$.

Therefore, a stronger convective loss occurs for sidebands with a higher $n_{//}$ gap from the pump, since both a stronger phase mismatching and a reduced overlap of the respective resonant cones are produced.

II.3. PUMP DEPLETION

In order to evaluate the amount of the RF power coupled by the antenna that is transferred by the PI to the sidebands, the non-linearly coupled WKB equations of pump

$$E_{1s}^2 \cong \frac{T_e}{4\pi\lambda_{De}^3}\frac{\omega_0}{\omega_{LH}}\sqrt{\frac{m_e}{m_i}} \tag{15}$$

and sideband should be considered. Following Ref. [16], for sideband wave originated by the thermal noise with electric field amplitude E_{1s},

$$\eta - \frac{E_{1s}^2 k_{\perp 0}}{2E_0^2 k_{\perp 1}} e^A \tag{16}$$

the fraction of pump power going to the sideband depends exponentially on the amplification factor and can be estimated by the following expression

As result, the amplification factor has a value A≈15 for sidebands with *n*//≈2.1÷2.3,

which corresponds to about 10% of pump power depletion. Since the inhomogeneity convective loss increase by increasing the $n_{//}$ gap of sideband and pump, a trend of monotonically decreasing pump depletion occurs at high $n_{//}$ (the is reduced to 0.1% for $n_{//} \approx 3$). Exceeding a certain $n_{//}$ threshold value ($n_{//\text{Sid-Cut-off}} \approx 3.5$) the sidebands cease depleting the pump, since its power density is insufficient for exceeding the threshold imposed by the convective losses (A>1). Finally, the trend of the fraction of the pump power transferred to the sidebands is plotted against the sideband $n_{//}$ in Fig.13, where also the respective trend of the amplification factor is shown. The error bar in the amplification factor depends on the uncertainty of the measured plasma parameters, which reflect in the determination of the growth rate (about 5%, from the data shown in Fig.7) and of the pump depletion (about 20%).

The results of both the frequency shift (≈a few hundred kHz) and the correlated pump depletion (≈10%) are consistent with the spectrum obtained by RF probe measurements shown in Fig.2.

Finally, the spectra launched by the antenna and broadened by PIs are shown in Fig.14. Therefore, due to the occurrence of the PI in the scrape-off plasma, we expect that the LH power spectrum penetrating in the bulk is significantly broader than the launched antenna spectrum. Such spectral broadening is important for determining the LH power deposition profile by the quasi-linear interaction with the electron distribution function. This aspect as been considered in Ref. [9,32].

IV. CONDITIONS FOR PRODUCING PI-INDUCED SPECTRAL BROADENING IN LOWER HYBRID CURRENT DRIVE EXPERIMENTS

In the previous section, the operating conditions have been determined for the occurrence at the plasma edge of a PI-induced spectral broadening in an important LHCD experiment of JET, which produced high electron temperatures, with broad profile, in the bulk [10-12,9]. In the present section, we discuss the general conditions for the occurrence of the spectral broadening in typical LHCD experiments. Such conditions have been obtained by means of analyses performed in a similar way as in Sec 3, which consider the operating parameters of different LHCD experiments (e.g., frequency, operating plasma density, antenna geometry, RF power density, confinement magnetic field, etc.).

As summary of the general results, the growth rate of the ion-sound-driven PI is significant (in the range $\gamma/\omega_0 = 10^{-2} - 10^{-3}$) by considering the whole range of operating frequencies (f_0 = 0.4GHz – 8GHz), coupled RF power densities (P_{LH} = 15MW/m^2 – 80MW/m^2), and operating line averaged plasma densities (from $n_e = 0.1\ 10^{20}$ m^{-3} to $1\ 10^{20}$ m^{-3}, which roughly correspond, respectively, to values ten times lower in the scrapeoff). The considered confinement magnetic field values are in the range: 1 – 6T.

In all the considered cases, the typical parameters relevant to the PI-driving quasimode are: $k_\perp \approx 10$ - 15cm^{-1}, $\omega/2\pi \approx 0.2 - 1$MHz. Such common behaviour is determined by the circumstance that all the LHCD experiments meet similar operating conditions, in the operating frequencies and scrape-off parameters, which determine mainly the growth rates and the launcher coupling performance as well. These conditions are: $n_{0//}$ in the range 1.5 – 3, and layers with $\omega_{pe}/\omega_0 \approx 1$ are located near the effective antenna-plasma interface (as necessary for launching the slow electron plasma wave); ω_{pe}/ω_0 of the order of ten, or more, in the layers close to the last closed magnetic surface, as typically obtained in JET and in other tokamaks as well [33,34]; the electron temperatures are in the range from a few eV to 100eV; the scrape-off radial dimensions lye typically in the range of 3 - 6cm.

Therefore, the PI-induced spectral broadening presented in the previous section (Fig.14) can be assumed as a characteristic of LHCD experiments performed in medium and large machines. Indeed the significant differences in the kinetic profiles (within about a factor two), which have been reasonably assumed in the scrape-off, result to not affecting significantly the growth rates. Such spectral broadening, besides the linear effects of wave propagation in toroidal geometry [7] should be considered in modelling the LH deposition profile, as was properly performed in Ref [9]. The modelling precision results to be enhanced by the fact that no cut-off occurs for ray propagations in the considered plasmas with high electron temperatures in the core ($\approx$7 – 10keV) and broad temperature profile ($\approx$ 3keV at two third of the minor radius).

We have considered the aforementioned link between the wave physics at the edge and in the bulk plasma, indicated by similar observations of diagnostic measurements of the edge, which are accompanied by a similar effect of successful or unsuccessful ingress of the coupled RF power in

the bulk (see Sec.2 and Appendix I). In particular, a significant ingress in the bulk of the coupled LH power was not compatible with the occurrence of a strong pump broadening. We have performed the calculation of the spectral broadening considering scrape-off layers slightly colder than the one described in Tab.I and Fig.5. The range of the considered electron temperature goes from T_e = 3(±2) eV to 30(±15) eV (in place of the range T_e = 10(±5) eV – 100(±50) eV in the analysis of Sec.3). It is reasonable considering appropriate such situation for early and recent LHCD experiments as well, performed in machines smaller than JET, and with electron temperatures in the core of the order of 1keV. However, the aforementioned considered conditions might apply also for experiments similar than JET (e.g., with similar parameters close to those of Tab.I), but operating with lower plasma currents and/or higher averaged densities. In this case, the obtained trend of LH spectral broadening is similar than the one shown in Fig.14, but with a slightly higher cut-off, at $n_{1//\text{Cut-off}} \approx 4 - 7$, (the upper limit corresponds to the lowest considered electron temperature). This behaviour is determined by the higher growth rates that allow further sidebands exceeding the convective threshold. The quasimode frequencies remain, instead, lying in the range of 0.2MHz –1MHz. The electron dynamics appears playing a dominant role in determining both the wellknown linear physics (i.e. the antenna coupling of the electron plasma waves, etc.) and the non-linear physics (i.e., the mode coupling producing PIs) relevant to the LHCD experiments. Indeed, in all cases, relevant to the scrape-off parameters of LH experiments, the condition of adiabatic electrons, $\omega \leq k_{//} v_{the}$, has been satisfied in solving the parametric dispersion relation, Eq.1. Such circumstance explains the growth rate behaviour, which results strongly dependent on the local electron temperature, as shown in Fig. 7 (and weakly dependent on the ion temperature). The higher growth rates that are produced by considering lower temperatures can be also explained in terms of the weak turbulence condition, which can be more easily met at relatively lower RF power densities and lower plasma energy contents.

Considering LHCD regimes at high operating plasma densities (so that the layers with $\omega_{pe} \gtrsim \omega_0$ and $\omega_{pi} << \omega_0$ are localised in the bulk), a further colder and overdense scrape-off layer is produced. Taking into account the aforementioned effect of the electron temperature on the growth rate, a more pronounced LH spectral broadening is produced. In these conditions, the effective LH spectrum penetrating in the bulk should be considered for modelling the LH deposition profile by the quasi-linear model. The results of such analysis are contained in a further work [32]. Due to the more pronounced spectral broadening expected to occur operating at higher plasma densities, the expected LH deposition profile occurs mostly more and more off-axis. In LHCD experiments operating at relatively high plasma densities, the obtained pretty low current drive efficiencies, accompanied by slightly stronger pump broadening of the RF probe spectra as well [31,28], are consistent with the related behaviour of the PIinduced spectral broadening.

For further higher operating plasma densities, so that $\omega_{pi} \approx 0.5\omega_0$, the occurrence of the ion tails observed in the early LH experiments can be interpreted as a phenomenon that originates at the plasma periphery, due to the enhanced Landau damping on both the electron and ion species that

the spectral broadening produces [32]. However, no clear evidence was provided that the ion tails observed in the so-called LH regimes at intermediate densities [24] were originated in the bulk, since the neutral particle diagnostics that were utilised for detecting the ion tails, are strongly sensitive to the physics of the scrape-off plasma. Finally, at the very high operating densities ($\omega_{pi} \approx \omega_0$) required by the early LH heating scheme of the bulk ions, the only evidence of the RF power interaction with the plasma resulted by the signatures in the RF probe spectra. These spectra might be actually interpreted in terms of a cascade of ion-soundquasimode- driven PIs (for the pump broadening) and ion-cyclotron-quasimode driven PIs, which reasonably inhibit the ingress of the coupled RF power in the bulk. Indeed, an enormous spectral broadening of the pump is produced for a very cold and overdense scrape-off layer and, consequently the LH deposition is localised at the very edge. Such hypothesis, formulated in Ref [21], is confirmed by the present analysis.

4. CONCLUSIONS

The conditions necessary for the occurrence of the spectral broadening induced by parametric instabilities are very close to those utilised for performing the LH power coupling to tokamak plasmas. These conditions present, indeed, equivalent plasma densities at the edge (considering the operating frequency), and similar cold and overdense scrape-off layers, with similar depth.

The PIs driven by ion-sound quasimode in the scrape-off plasma of LHCD experiments are expected producing, at the routinely coupled RF power densities ($> 10MW/m^2$), a spectral broadening that consists in the depletion of a small fraction of the launched RF power (≈10%). As effect of the convective losses due to the plasma inhomogeneity and finite extension of the pump, by increasing the $n_{//}$ shift of the sidebands with respect the launched $n_{//}$ peak of the pump, the power depletion vanishes above a certain $n_{//}$ threshold of sideband, which results higher considering higher plasma densities and/or lower electron temperatures. In the LHCD experiments, which typically operate with a peak $n_{//} < 2$, electron temperatures in the scrape-off ranging from a few eV to a hundred eV, and plasma densities determined, given the other parameters, mainly by the operating averaged density (roughly: $n_{eLCMS} > 0.1 n_{eAverage}$), the resulting $n_{//}$ cut-off of the LH spectrum penetrating in the bulk is about 1.5 times the launched $n_{//}$ peak. The relevant quasimodes have typically $k_\perp \approx 10$ - 15 cm^{-1}, and frequencies in the range (0.2MHz - 1MHz) consistent with the measured spectra of the density fluctuations at the edge, and the RF probe pump broadening as well.

The consideration of the inferred spectral broadening allows producing consistent interpretation of the linked phenomenology of the LH physics at the edge and in the bulk plasma, which occurs in the different tokamak scenarios utilising externally launched LH waves. Regarding the effects produced in the plasma bulk, the consideration of the PI-induced spectral broadening in modelling the deposition profile in LHCD-sustained ITBs of JET [10-12,9], produced a consistent interpretation of the available experimental results, especially in plasmas with high central electron temperatures (≈7 –10keV) and broad temperature profile (≈ 3keV at two third of the minor radius) [R Cesario, et al., PRL **92** 17 (2004) 175002]. In addition, in the LH experiments that were aimed at heating the

bulk ions, which required relatively high plasma densities of operation, the PIs are expected producing a stronger spectral broadening, which is consistent with both the more and more pronounced pump broadening in the RF probe spectra, and the further off-axis LH deposition profile, which becomes fully stopped at the edge for higher plasma densities.

Therefore, the aforementioned linked physics of the edge and main plasma, indicated by the different density regimes of the LH experiments, can be provided by the Landau damping on the plasma species, via the $n_{//}$ spectral broadening produced by the PIs, besides the effects of ray propagations. Considering the cooperation of both the effects of PIs and toroidal geometry ray propagation in determining the spectral broadening, a more precise LH deposition profile is modelled, especially in plasmas with high central electron temperatures with broad profile. It is due to the absence or negligible wave cutoff occurrences, which do not make worse the precision of the LH deposition profile [R Cesario, et al., PRL 92 17 175002 2004, Castaldo et al. to be pub.].

The spectral broadening results weakly dependent on the minor changes of the measured scrape-off profiles (which have typically $T_{\text{e Average}} \approx 20\text{eV}$) due to the experimental uncertainties (roughly a factor two). Conversely, the broadening might be significantly reduced operating with warmer scrape-off ($T_{\text{e Average}} > 50\text{eV}$), possibly, in Litium-coated vessel [38,39]. If verified, such circumstance is important since the LH deposition profile might be determined by the antenna spectrum more clearly than in the present experiments (e.g., see Ref. [40]).

Operating with warmer and less dense scrape-off layers in tokamak plasmas, a proper tailor of the launched $n_{//}$ antenna spectrum (electronically achievable) would possibly allow performing a further control of the LH deposition and the magnetic shear profiles in the plasma.

The consideration of the proposed mechanism of spectral broadening should allow a precise modelling of the LH-driven current density profile, which is useful for designing experimental scenarios that require the control of the current profile by means of lower hybrid waves. This argument is deeply discussed in a companion paper [32].

APPENDIX I

In the present Appendix, a summary of the phenomenology of the physics of the edge observed during the LHCD experiments on ASDEX is given, as shown in Ref [22].

A broadening of the density fluctuation was detected by microwave reflectometry, in combination of an analogous spectral broadening of the RF probe signal, was observed, see Fig A1. A more pronounced spectral broadening occurred when a certain RF power threshold was exceeded, lower at higher operating plasma densities, thus suggesting that a non-linear phenomenon at the plasma edge should drive the phenomenology of the spectral broadening. Consistently with the results of ASDEX, some spectral broadening of the plasma density fluctuations is found during coupling of LHCD power on JET.

The study for ascertaining the origin of the pump broadening occurring in the lower hybrid current drive experiments, was performed utilising both the RF probe and microwave reflectometry

of the plasma edge measurements. As result, a trend of the spectral broadening with the coupled LH power was found, which indicated the occurrence of some non-linear interaction of the launched LH waves with the plasma density fluctuations at the edge. As higher was the operating plasma density, lower resulted the minimum RF power necessary for producing a pronounced spectral broadening.

The role of the parametric instability in producing the spectral broadening was excluded in the analysis results related in Ref [22]. A deeper consideration of such analysis has shown that such conclusion is wrong, since a complete computation of the growth rate in the more realistic interaction layer, which involves the whole scrape-off layer, was not carried out. The utilised numerical tool utilised in the work was not adequate for considering plasma layers sufficiently close to the antenna-plasma interface (at $\omega_{pe} \approx \omega_0$), in which the growth rates of the ion-sound-quasimode-driven PIs become dominant. As consequence the absolute maximum of the growth rate was not found, and the threshold of RF power density of parametric instability was estimated to be much higher than the RF power densities utilised in the experiment. The recent progress performed with the tool for the parametric instability model makes possible to determine more properly the trend of the growth rate in the whole scrape-off, the spatial amplification factor and the pump depletion. Therefore, the model shown in the present paper is able to interpret the common phenomenology of the RF probe and the microwave reflectometry signals utilising the same framework of the parametric instability, as shown in Sec. 2 and Sec. 3. The frequency of the quasi-mode driving the instability is in the same range (0.2MHz – 1MHz) of the spectral broadening of both the plasma density fluctuations and the RF line broadening.

APPENDIX II

In the present appendix, we summarise the calculation performed for checking that the PI wavevector components resulting from the numerical analysis performed considering realistic plasma parameters of the LHCD experiment of Tab. I are consistent with the condition: $Mx \approx k0x\text{-}k1x$ which has been derived in the Sec 3.2 (Eq.4).

The plasma density radial profile as been assumed as:

$$\eta - \frac{E_{1s}^2 k_{\perp 0}}{2E_0^2 k_{\perp 1}} e^A$$

where n_{e0} is the density at the layer $\omega_{pe} \approx \omega_0$ with a high growth rate (see Sec. 3.1). Such layer is located at the interaction point $x = 0$, close the antenna-plasma interface. The characteristic density length $\lambda \approx 1$cm can be assumed for scrape-off of tokamak plasmas. Eqs.5 have been solved for typical spectrum launched by an LHCD antenna ($n_{0//Peak} = 1.85$, $\Delta n_{0//} = 0.2$) and for a sideband with which has a reasonably small $n_{//}$ gap from the pump ($n_{1//} = 2.1$). As result, a phase mismatching $M_x \approx 0.24\text{cm}^{-1}$ is obtained at a layer located 1cm away from $x = 0$. Such mismatching is lower than the minimum mismatching of 0.2cm^{-1} and, therefore, it is verified that the considered low frequency perturbation produces coupled modes consistent with the instability scalelength.

ACKNOWLEDGEMENTS

The authors acknowledge Dr F. Santini for the very helpful discussions.

[1]. N.J. Fisch, Phys. Rev. Lett. **41** (1978) 873

[2]. S. Bernabei, et al., Phys. Rev. Lett. **49**,2 (1982) 1255

[3]. N.J. Fisch, Rev. Mod. Phys, **59**, (1987) 175

[4]. F. Santini in Course and Workshop on Applications of RF waves to Tokamak Plasmas, Varenna (Italy) 1985, Editors, S Bernabei, U. Gasparino and E. Sindoni, International School of Plasma Physics (1985) 251

[5]. M. Brambilla, Kinetic Theory of Plasma Waves, Clarendon Press, Oxford (1998) 551-552 -557

[6]. S. Succi, et al. Proc. Of the 10th Int. Conf. On Plasma Physics and Controlled Nuclear Fusion Research, London, 1984 IAEA, Vienna, Vol. I, 549

[7]. P.T. Bonoli, Englade R.C., Phys. Fluids, **29**, 2937 (1986)

[8]. G. Giruzzi, et al., Nucl. Fusion **37**(5), (1997) 673

[9]. R. Cesario, et al., PRL **92** 17 (2004) 175002

[10]. J. Mailloux, et al., Phys. of Plasmas, **9**,5, (2002) 2156

[11]. F. Crisanti, et al., Phys. Rev. Lett., **88** (2002) 145004

[12]. C. Castaldo, et al., Phys. of Plasmas, **9** 8 (2002) 3205

[13]. M. Porkolab, Phys Fluids **17** ,1432 (1974)

[14]. M. Porkolab, Phys Fluids **20** 2058 (1977),

[15]. C.S. Liu in Advance in Plas. Phys, Edit. by A. Simon and W.B. Thomson, (Wiley, New York 1976) Vol. 6 p. 121M. Porkolab, Phys Fluids **20** 2058 (1977)

[16]. L. Chen, R. and L., Berger, Nucl. Fusion **17,** 779 (1977)

[17]. V.K. Tripathi, C.S. Liu and C. Grebogi, Phys. Fluids **22**, 1104 (1979)

[18]. E. Villalon, and A. Bers, Nucl. Fusion, 20243 (1980)

[19]. C.S. Liu and V.K. Tripathi Phys. Fluids Report **24**,1709 (1984)

[20]. Y. Takase, et al. Phys. Fluids **26**, 2992 (1985)

[21]. R. Cesario and A. Cardinali, Nucl. Fusion **29**, 10 , 1709 (1989)

[22]. R. Cesario, et al., Nucl. Fusion, **32**, 2127 (1992)

[23]. R. Cesario, et al., Nucl. Fusion, **11**, 261 (1994)

[24]. F. De Marco in Course and Workshop on Applications of RF waves to Tokamak Plasmas, Varenna (Italy) 1985, Editors, S Bernabei, U. Gasparino and E. Sindoni, International School of Plasma Physics (1985) 316

[25]. R. Cesario and V. Pericoli, Nucl. Fusion (1987)

[26]. P.I. Andrews and F.W. Perkins, Phys. Fluids **26** (1983) 2546 and 2537

[27]. Y. Ikeda et al., Nucl. Fusion Vol. 34, n.6 (1994)

[28]. V. Pericoli-Ridolfini, A. Ekedahl et al, Plasma Phys. Contr. Fus. 39 (1997) 1115

[29]. V. Pericoli-Ridolfini et al, to be published

[30]. F. Alladio et al, et al., at the 15th European Conf. on Controlled Fusion and Plasma Heating, Dubrovnik, May 1988, Edited by J. Heijn Petten, European Physical Society 1988 Vol 12B part III, p. 878

[31]. R. Cesario et al., at the 15th European Conf. on Controlled Fusion and Plasma Heating, Dubrovnik, May 1988, Edited by J. Heijn Petten, European Physical Society 1988 Vol 12B part III, p 896

[32]. Castaldo et al., to be pub.

[33]. V. Pericoli-Ridolfini, et al., Journal of Nuclear Materials 20 (1995)

[34]. M. Leigheb et al., .Journal of Nuclear Materials 914 (1995)

[35]. S. Hacquin, L. Meneses, L. Cupido, N. Cruz, L. Kokonchev, R. Prentice, C. Gowers and the JETEFDA contributors, 15th Topical Conference on High-Temperature Plasma Diagnostics, San Diego, April 2004

[36]. E. Mazzucato, Nucl. Fus. 41 203 (2001)

[37]. R.L. Berger, et al, Phys. Fluids 20 1864 (1977)

[38]. M. Abdou, et al., Fus. Eng. Design,. **54**, 181 (2001)

[39]. S.I. Krasheninnkov, L.E. Zakharov, G.V Pereverzev Phis. of Plasmas, **10** 1678 (2003)

[40]. Ide et al. at the IAEA 2004

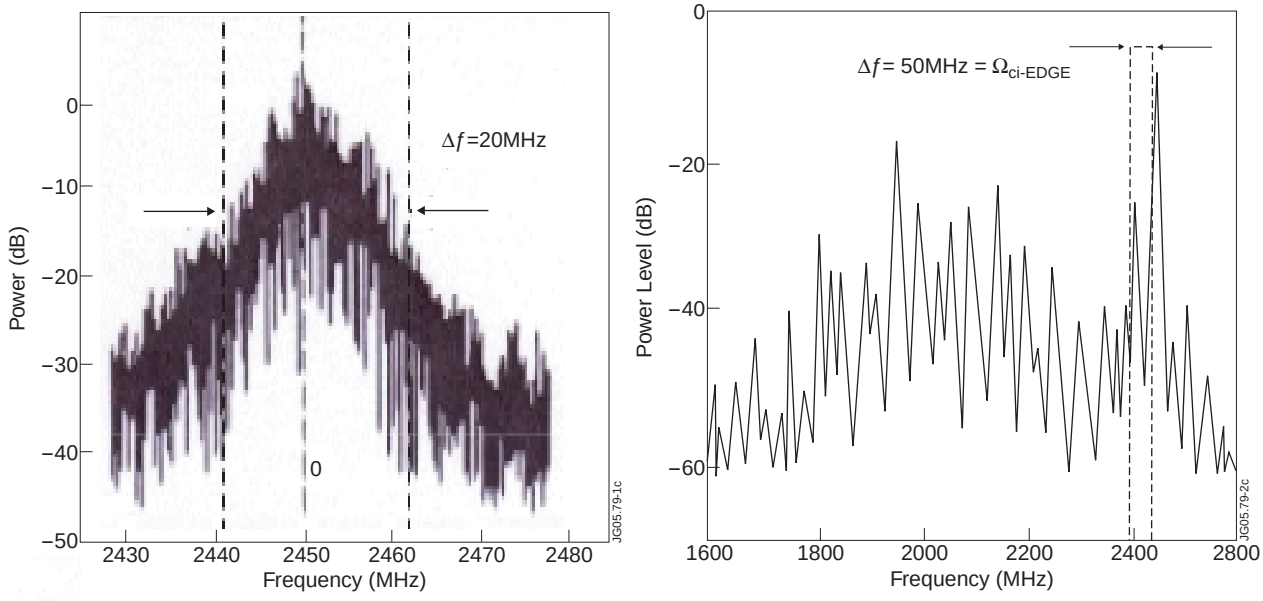

Figure 1: a) RF probe frequency spectrum typically obtained during LH experiments aimed at heating the ions on the FT tokamak around the operating frequency (from Ref. [21,25]). The pump broadening is measured 10dB below the power peak (excluding the operating frequency line width due to the RF power generator).

b) Same frequency spectrum as in Fig. 1a, but over a broader spanned frequency. The sidebands shifted by the ion-cyclotron frequency of the plasma edge exhibit the typical non-monotonic envelope.

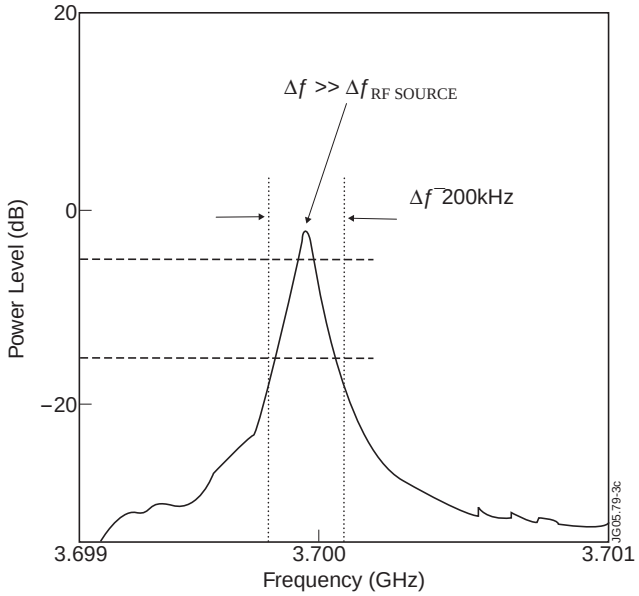

Figure 2: Typical spectral broadening from a RF probe located inside the main vessel during an LHCD experiment of JET, Pulse No: 35021 at t=5.40s – 5.45s, $P_{LH} \approx 5MW$ $n_e \approx 1\ 10^{19}\ m^{-3}$, $B_T \approx 3T$, $I_P \approx 3MA$, $n_{//peak} = 1.84$.

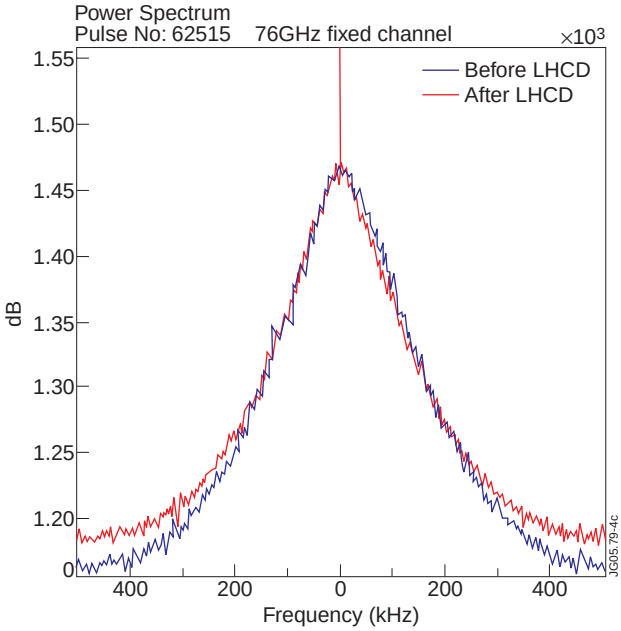

Figure 3: Comparison of the spectra of the reflectometry signal before (5.0 - 5.7s) and during (5.7 - 6.4s) the LHCD phase of an experiment of JET utilising 2MW of LH power in combination of the main heating phase (neutral beam injection and ion cyclotron resonant heating, Pulse No: 62515). A similar broadening of the density fluctuation spectrum is observed operating in different conditions of plasmas utilising LHCD.

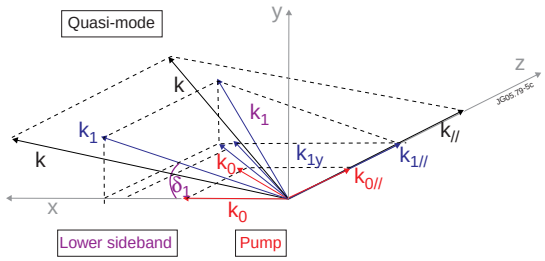

Figure 4. Slab geometry and wavevectors of the coupled modes.

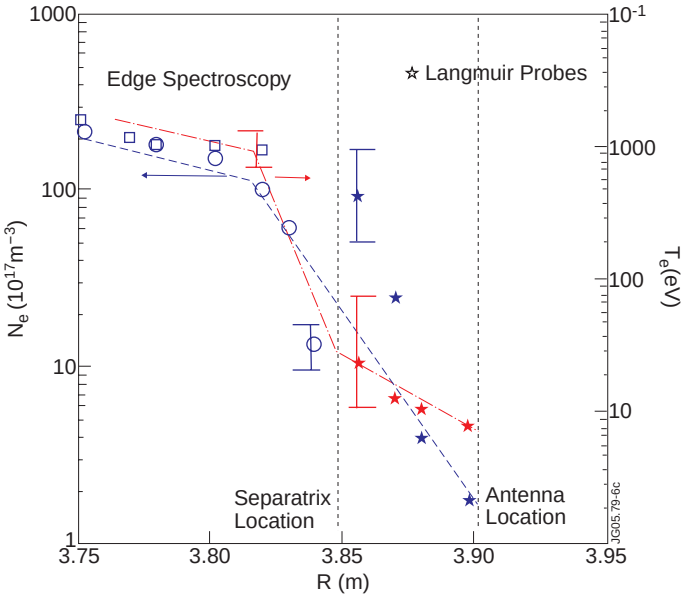

Figure 5: Profiles of the plasma density and of the electron temperature of the scrape-off-layer utilised for the analysis. The same LHCD experiment of JET of Tab. 1 is considered (Pulse No: 53429 during the LHCD phase, at t = 46s). The star symbols refer to Langmuir probes (for density and electron temperature), the circles refer to the density and the squares to the electron temperature measured with the spectroscopy of the edge.

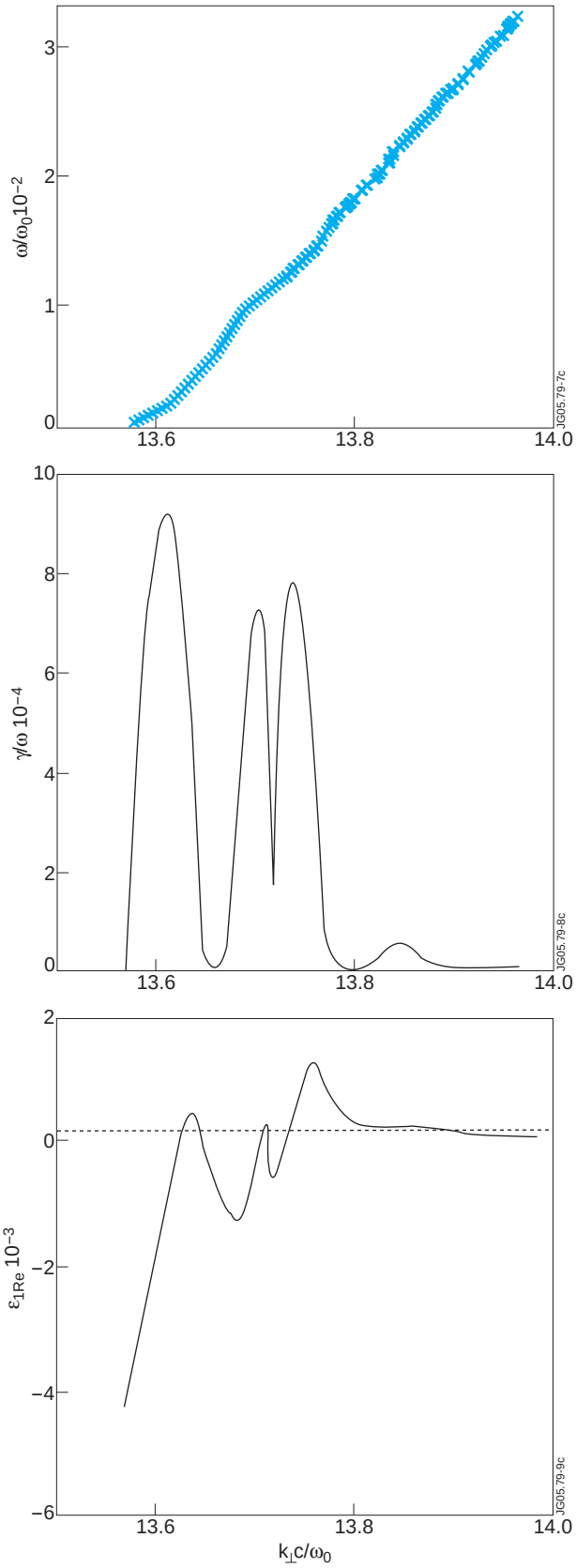

Figure 6: Trend of the frequency and the growth rate of the low frequency mode which drives the instability plotted versus the perpendicular wavenumber of that mode. The parameters of Tab.1 and a set of parameters roughly occurring in the middle of the scrape-off plasma layer (see Fig.5) have been considered (n_e *= 1* 10^{18} m^{-3}, T_e *= 30eV, RF power density 1MW/*m^2*).*

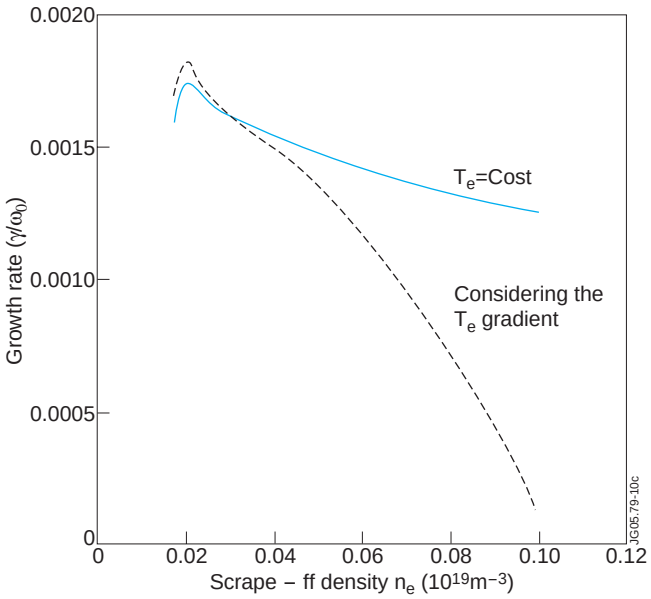

Figure 7: Behaviour of the growth rates maximised with respect to $k_\perp$, plotted against the local plasma density. The different behaviours are compared by keeping the electron temperature constant (30eV, continuous curve), and changing accordingly with the scrape-off profile of Fig.5 (dashed curve). Other parameters as in Tab. 1.

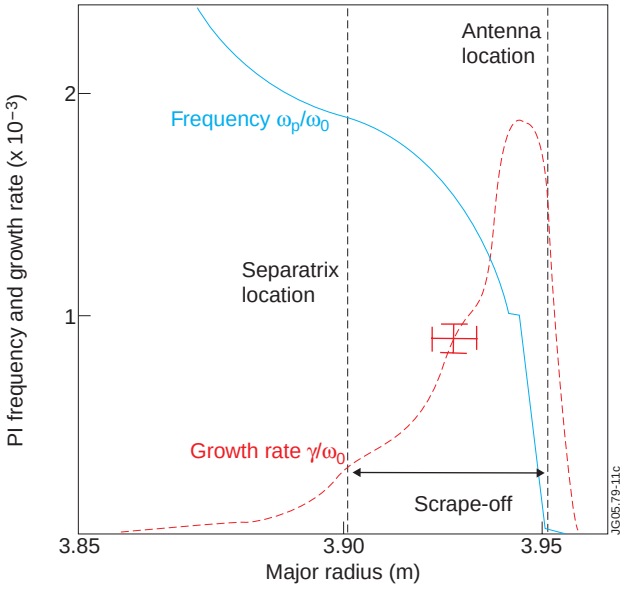

Figure 8: Growth rates of the quasi-mode-ion-sound-driven parametric instability maximised with respect to $k_\perp$ plotted versus the major radius. The scrape-off layer between the launcher mouth and the separatrix is indicated. Same parameters as in Fig.7.

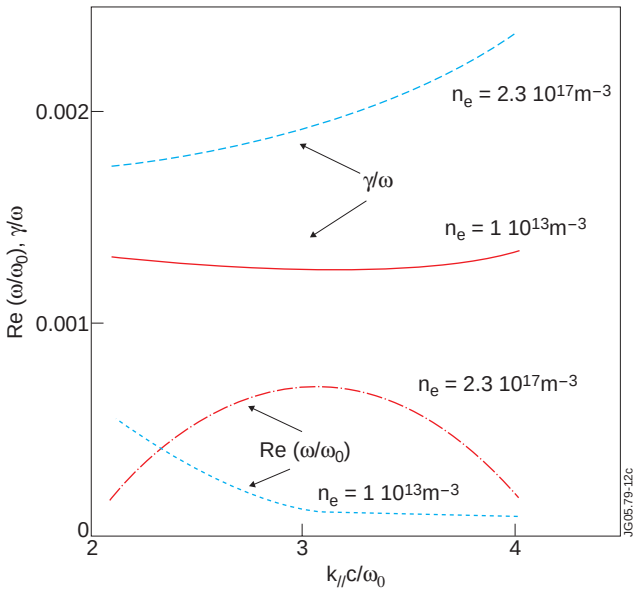

Figure 9: Trend of the growth rate with respect to the parallel refractive index of the sidebands. Same parameters of Fig.7.

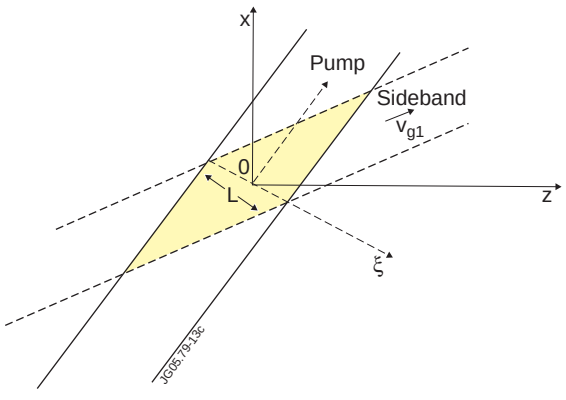

Figure 10: Scheme of the LH resonant cone regions in the scrape-off of the pump and LH waves.

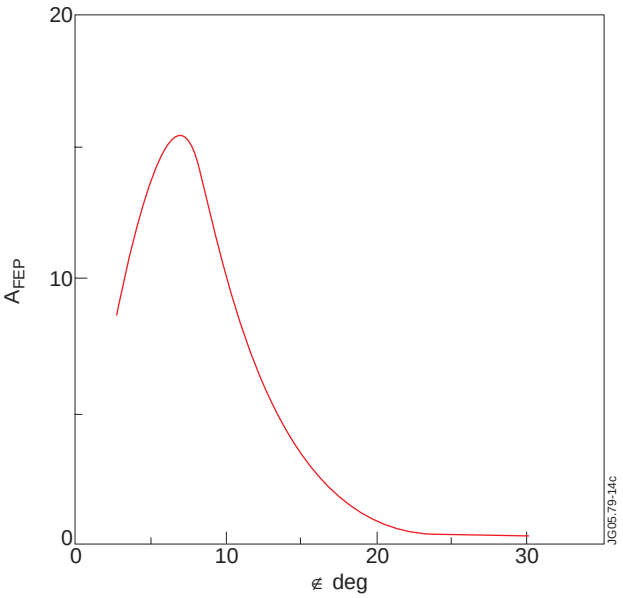

Figure 11: Behaviour of the amplification factor, maximised with respect to the quasi-mode $k_{\perp}$ *with respect the angle* $\delta_1 = \angle(\mathbf{k}_{1\perp}, \mathbf{k}_{0\perp})$. *Same parameters of Fig.7.*

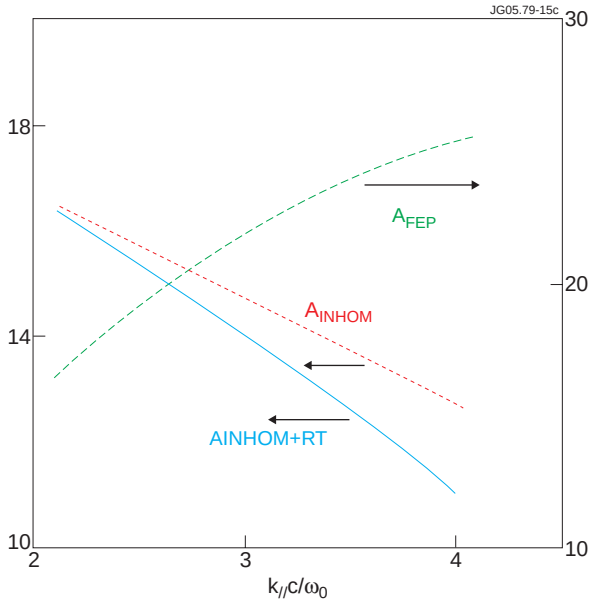

Figure 12: Plots of the functions A_{FPE}, A_{INHOM} *versus the parallel refractive index of sideband. Same parameters of Fig.7.*

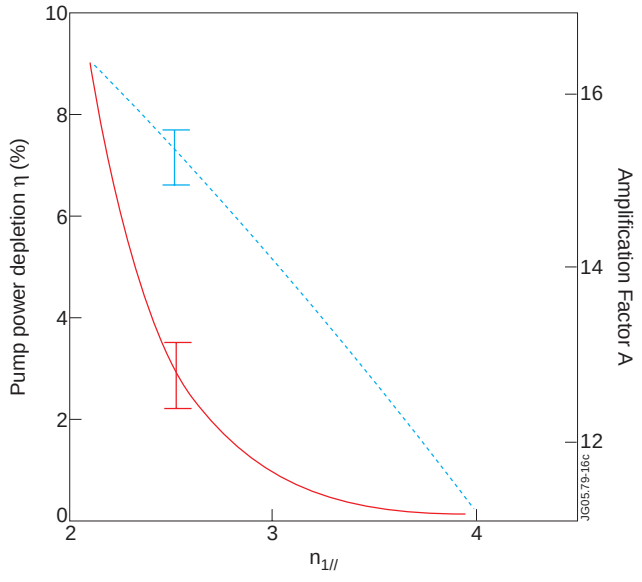

Figure 13: Trend of the depletion of the LH pump power with the parallel refractive index of the sideband. Same parameters of Fig. 7.

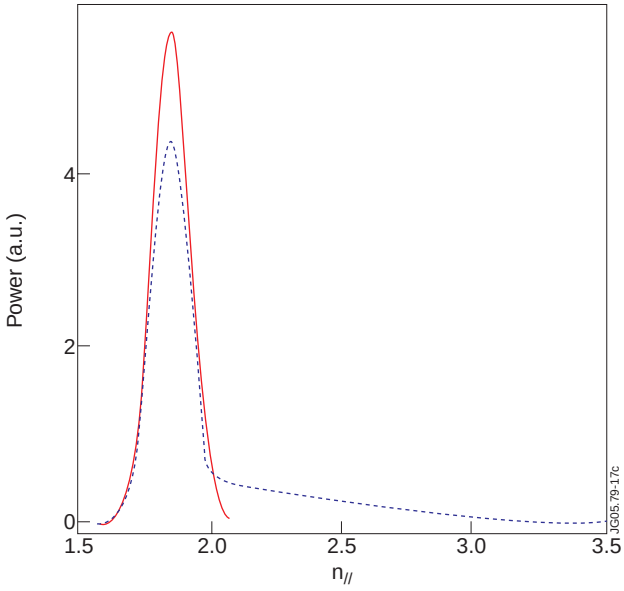

Figure 14: Comparison of the LH power $n_{//}$ *spectrum launched by the antenna (dotted curve) and expected penetrating in the plasma bulk by the effect of the parametric instability (dashed curve). Same parameters of Fig. 7.*

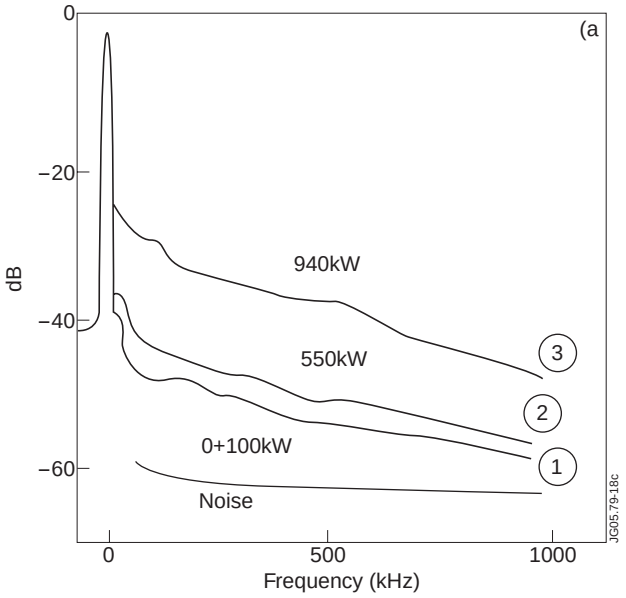

*Figure A1: Reflectometry of the edge during LHCD in ASDEX, from R. Cesario, et al., Nucl. Fusion, **32**, 2127 (1992).*